

Preparation, Characterization and Application of Mixed Clay Based Low-Cost Ceramic Membrane in Treatment of Oil-in-Water Emulsions

Kanchapogu Suresh^{a*}, Amish Gour^a, Mukesh Kumar Yadav^b, Vidhi Jani^c,

^{a*, a,b,c} Department of Chemical Engineering, Maulana Azad National Institute of Technology Bhopal-462003, India
^{*}Corresponding author Dr. Kanchapogu Suresh, ksuresh@manit.ac.in, +91 755-405-1807

Abstract

Fly ash is a cost-effective alternative for preparing ceramic membranes but they are often weak for practical use. We have made different mixtures by taking different compositions of polyvinyl alcohol to improve mechanical strength at the same time preserving permeability. We tested 3 PVA concentrations from which sintered 10 ppm PVA solution treated at 1100 °C demonstrated optimal characteristics, featuring L_h (water permeability coefficient) of 9.19×10^{-6} ($m^3/m^2 \text{ s kPa}$), 39% porosity, pore size of 1.029 μm , a flexural strength of 40 MPa, and testing with oil-in-water emulsions revealed a rejection rate exceeding 98%.

Keywords: Cost-effective; Fly ash; Pore-forming agent; Ceramic membrane; Wastewater.

1. Introduction

Ceramic membranes have gained widespread use in wastewater treatment due to their specific attributes, including high flux, antifouling properties, extended lifespan, and operational flexibility [1]. Primarily made from various raw ingredients such as kaolin, titania, alumina, and silica, zirconia. Generally, ceramic membranes exhibit exceptional mechanical, chemical and thermal stability in contrast to polymeric alternatives, enduring pressures and high temperature effectively. They are robust and

can be cleaned using strong industrial chemicals without notable performance degradation [2]. Recent studies have emphasized cost reduction through the use of economical raw materials such as kaolin, clay, and fly ash, sintered at lower temperatures (1100°C). Kaolin, a widely available and cost-effective clay mineral, is commonly employed in ceramic membrane production [3].

While kaolin-based membranes dominate the literature, some scholars have explored using

fly ash as a free raw material to produce inorganic membranes, aiming to further reduce costs. However, fly ash-based membranes exhibit wider pores, lower porosity, and inferior strength compared to their kaolin-based counterparts. Combining fly ash and kaolin could yield cost-effective membranes with favorable physical and pore properties [4]. Despite this, there is a lack of published studies on inorganic membranes created from fly ash and kaolin mixtures.

This study evaluated the mechanical strength of fly ash ceramic membranes using a compression machine and assessed membrane chemical stability with Hydrochloric acid (0.1M) and Sodium Hydroxide over seven days. Surface characteristics were analyzed using a field emission scanning electron microscope [5]. Previous studies by Singh et al. (2020), Liu et al. (2019), Yu et al. (2018), Wang et al. (2018), and Zhao et al. (2016) emphasized the favorable attributes of fly ash-based ceramic membranes, such as exceptional mechanical strength, high water permeability, efficient contaminant removal, and long-term stability [6-10].

Despite advancements, certain research gaps remain, including evaluating the economic viability of large-scale water treatment using ceramic membranes. The cost-effectiveness of the fabrication process, encompassing material procurement, fabrication, and operation, requires further investigation. Additionally, limited knowledge exists regarding the performance of ceramic membranes under various water quality circumstances. Most current research focuses on ideal conditions, necessitating more studies on real-world scenarios with varying organic and inorganic impurities in wastewater. Efficient cleaning and regeneration techniques for fly ash-based ceramic membranes are also crucial to address fouling issues [11-12].

The objectives of this research are as follows:

- a) Develop ceramic membranes from mixed clays using the uniaxial pressing method.
- b) Characterize the fabricated ceramic membrane through Archimedes' principle, chemical analysis, mechanical testing, and SEM.
- c) Apply the fabricated membrane for separating oil-in-water emulsions via dead-end microfiltration.

2. Materials and Methods

2.1. Compounds Used

2.1.1. Fly Ash

Fly ash is a finely divided material that is produced as a byproduct from the combustion of coal in power plants and carried away by flue gases. This pulverized fuel ash contains mineral components such as silica, alumina, and calcium oxide. Its remarkable pozzolanic properties have made fly ash a valuable resource in the construction industry, enhancing the strength and durability of concrete. Beyond its role in construction, fly ash finds applications in diverse fields, including agriculture, road stabilization, and even as a raw material in the creation of ceramic membranes. Importantly, the utilization of fly ash in various industries contributes to sustainable practices by diverting a substantial waste stream away from landfills. The specific constituents of fly ash are influenced by the variety of coal, as illustrated in Table 1.

Table 1. Fly ash composition by coal type

Component	<i>Bituminous</i>	<i>Subbituminous</i>	<i>Lignite</i>
Al ₂ O ₃ (%)	15-30	24-28	21-24
CaO (%)	5-10	10-20	20-35
Fe ₂ O ₃ (%)	15-30	5-8	5-12
SiO ₂ (%)	30-50	42-58	20-40
LOI (%)	0-10	0-2	0-6

2.1.2. Quartz

Quartz, a resilient and crystalline mineral, is primarily composed of silica, also known as silicon dioxide. In this mineral, each oxygen atom is shared between two tetrahedra, forming a continuous framework of SiO₄ silicon-oxygen tetrahedra. This arrangement gives quartz its chemical formula, SiO₂. Following feldspar, quartz stands as the second most prevalent mineral in the Earth's continental crust. Both normal and high-temperature quartz are recognized as two chiral forms of this mineral [13].

2.1.3. Kaolin

Aluminium silicate minerals, such as feldspar, undergo chemical weathering processes that lead to the creation of kaolinite, characterized as a soft and earthy mineral typically exhibiting a white color. The term "China clay" or "kaolin" is used to describe rocks with elevated concentrations of kaolinite and halloysite [13].

2.1.4. Boric Acid

Orthoboric acid, with the chemical formula B(OH)₃, is a chemical compound composed of boron, oxygen, and hydrogen. It is alternatively known as trihydroxidoboron, hydrogen orthoborate, and boracic acid. Found naturally as the mineral sassolite, orthoboric acid is

commonly encountered in the form of colorless crystals or a white powder that readily dissolves in water. As a weak acid, it can engage in reactions with alcohols, yielding borate esters, along with the formation of various borate anions and salts.

2.1.5 .Calcium Carbonate

Calcium carbonate, identified by the chemical formula CaCO_3 , is a common compound found in nature. It is prevalent in rocks as the minerals calcite and aragonite, with limestone being a notable example. Limestone, a predominant type of sedimentary rock, is primarily constituted by calcite [13].

2.1.6 .Titanium Dioxide

Titanium dioxide, or TiO_2 , functions as a versatile white pigment extensively employed in industries like paints, coatings, and cosmetics due to its outstanding light-scattering capabilities. It adds brightness and opacity to diverse products. Widely utilized in sunscreens for UV protection, titanium dioxide's inert and non-toxic characteristics make it a favored option in applications ranging from food coloring to photocatalysis.

2.2 .Method of membrane fabrication

The raw precursors used for the disc-shaped membrane from fly-ash are detailed in Table 2, and the specific quantities of each individual raw material are illustrated in Figure 1. Fly ash is collected from a power plant, and then it is sieved to remove impurities such as stones, metals, and other particles. The fly ash is then washed and dried to remove any impurities and moisture. A mixture is prepared by mixing fly ash, sodium metasilicate, quartz, kaolin, boric acid, calcium carbonate and titanium dioxide in a fixed ratio. Three solutions are prepared with different concentrations of PVA: 2 ppm for sample S1, 5 ppm for sample S2 and 10 ppm for sample S3 and water is added as binder to the mixture. The components are thoroughly mixed and kneaded to get a mixture of uniform composition [13]. The slurry is then placed in a casting mould and pressed under a pressure of 400 KN to obtain disc shaped membrane [13]. The membrane is first dried under sun for 24 hours. Then it is sintered in the muffle furnace in the following fashion [shown in Fig.2]: The programme of programmable furnace

1. To attain a temperature of 100°C , a time of 45 mins is set. The temperature of 100°C is held for a duration of 1440 mins (1day).
2. To attain a temperature of 200°C , a time span of 60 mins is provided. The

temperature of 200°C is held for a duration of 1440 mins (1day).

- To attain 1100°C of temperature, a time duration for 540 mins is provided. The attained temperature is held for 300 mins. The final obtained sintered membrane shown in Fig.3.

The systematic overall procedure followed for membrane preparation was depicted in Fig.4.

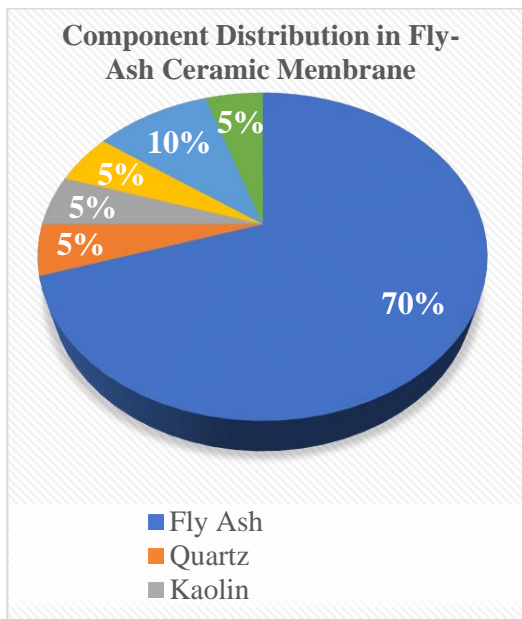


Figure 1: The distribution of components utilized in membrane



Figure 2: Sintering of membrane in muffle furnace



Figure 3: Ceramic Membrane after sintering in muffle furnace

Table 2. Ingredients used for manufacturing of membranes S1, S2 and S3

Component	Weight (in grams)
Fly Ash	70
Quartz	5
Kaolin	5
Boric Acid	5
Calcium Carbonate	10
Titanium Dioxide	5

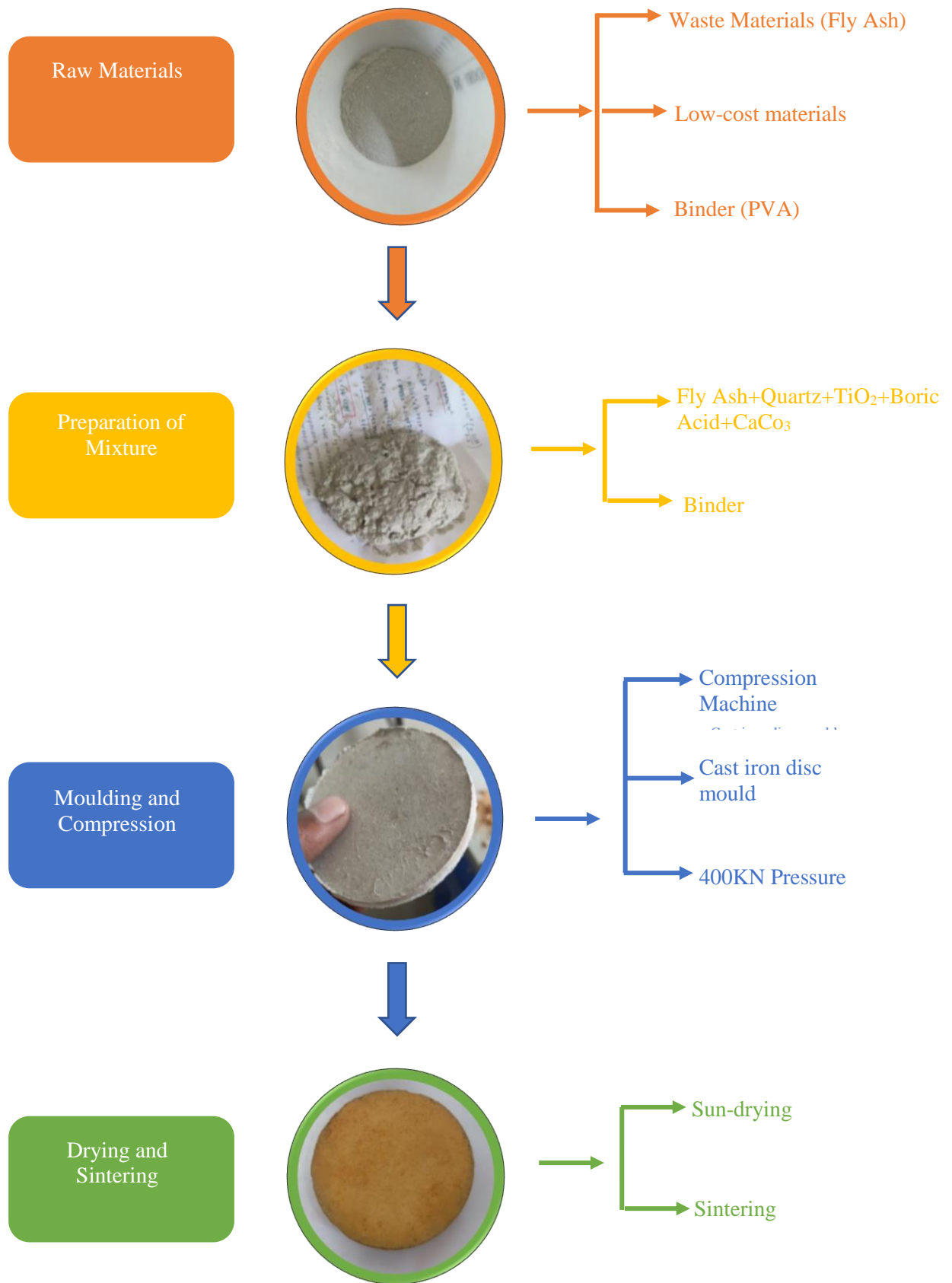


Figure 4: Process Chart for the Preparation of Ceramic Membrane

3. Results and Discussion

3.1 .Porosity

The membranes are submerged in a water container for a duration of 24 hours, after which it is weighed, and the following equation (equation 1) is employed to calculate the porosity.

$$\text{Porosity} = \frac{w_2 - w_1}{w_2} \times 100 \dots \dots \text{Equation (1)}$$

Where w_1 is the weight of the membrane before experiment and w_2 is the weight of the membrane after experiment.

Porosity results for the three membranes are presented in Table 3.

Table 3. Porosity results through Archimedes principle for S1, S2 and S3

Membrane	Porosity	SEM Analysis Porosity
S1	20%	25
S2	24%	30
S3	39%	45

The membranes exhibit a maximum porosity of 39%.

3.2. Surface Morphology

The sintered membrane was analyzed using scanning electron microscopy (SEM), and the corresponding image is presented in Fig. 5.

These images reveal the surface of the membrane, showing a rugged morphological structure. The SEM images verify that the membrane surface is devoid of cracks or pinholes, indicating a defect-free surface.

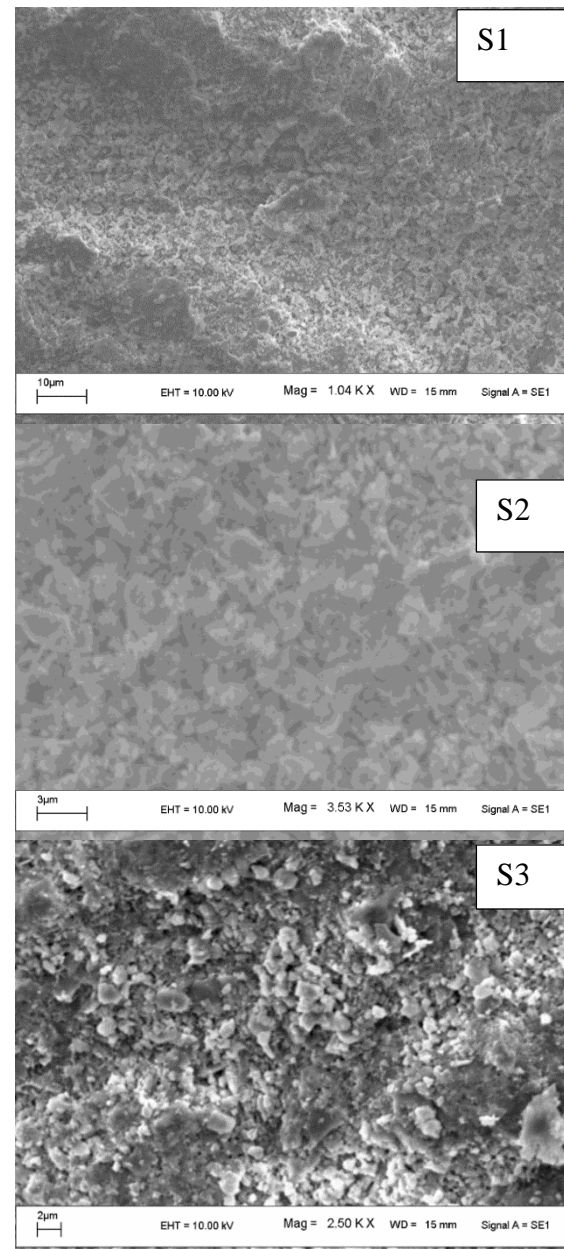


Figure 5: SEM micrograph of membrane S1, S2, S3 respectively

Furthermore, the membranes' average pore diameter is determined through SEM image analysis by employing ImageJ software [14].

The membranes' S1, S2 and S3 pore size has been measured and reported as average value, represented as d_{avg} , is computed using the equation 2 below:

$$d_{avg} = \sqrt{\frac{\sum_{i=1}^n n_i d_i^2}{\sum_{i=1}^n n_i}} \dots \dots \text{Equation (2)}$$

d_{avg} represents the average pore diameter in micrometers (μm).

From SEM images, The membranes' S1, S2 and S3 pore size has been measured and reported as average values of 2.7 μm , 2 μm , and 1.59 μm , respectively.

3.3. Chemical stability

Membranes' chemical stability was evaluated by exposing them to acidic and basic environments by calculating individual membrane weight loss. The membranes were kept in strong acid (HCl) and base (NaOH) solutions for one week to assess their stability in acidic and basic environments. The weight loss in terms of the percentage of the membranes was determined by comparing their dry weights before and after exposure to the solutions using Equation 3. The resulting

chemical stability data for the membranes are summarized in Table 4.

$$\text{Weight loss(\%)} = \frac{(W_1 - W_2)}{W_1} \times 100 \text{ Equation (3)}$$

Table 4. Observations for chemical stability of membranes S1, S2 and S3

Membrane	Initial weight (g) in		Final weight (g) in		Weight loss (%)	
	Acid	Base	Acid	Base	Acid	Base
S1	16.23	16.08	13.50	14.22	16.8	11.5
S2	16.52	15.95	12.15	14.11	26.4	11.5
S3	16.85	16.11	14.41	15.11	14.5	6

According to the findings, the membranes demonstrate superior corrosion resistance in alkaline conditions [13].

3.4. Mechanical strength

For effective utilization in ultra- and nanofiltration applications, a desirable ceramic



Figure 6: Sample placed in a Hydraulic Press

membrane should possess high mechanical strength, ideally exceeding 30 MPa [4]. To mitigate errors, we subjected three membranes individually to examination in a hydraulic press, as illustrated in Figure 6.



Figure 7[a]: Membrane S1, Yield Load(kN):5.92 Yield Stress (MPa):26.311

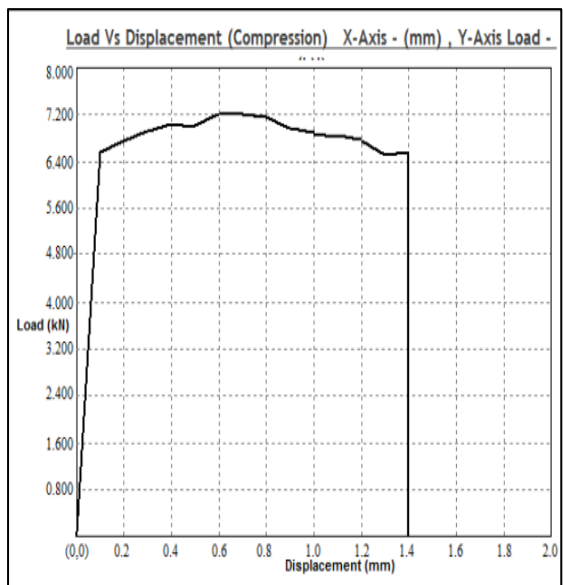


Figure 7[b]: Membrane S2, Yield Load (kN):6.52, Yield Stress (MPa):28.978

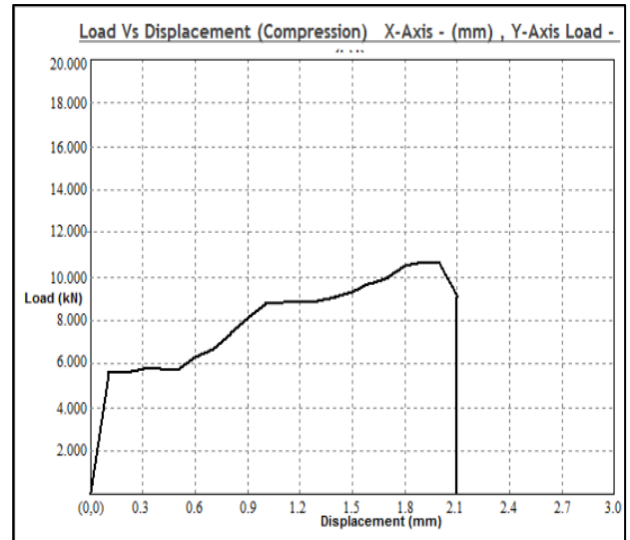


Figure 7[c]: Membrane S3, Yield Load (kN):8.84, Yield Stress (MPa):39.289

Figure 7: Mechanical strength of membrane through Universal Testing Machine (UTM).

From Fig 7. (a) To Fig.7. (c) The tested mechanical stability curve depicted through that the mechanical strength of the membrane was calculated. The strengths of membrane S1, S2 and S3 has been obtained as 26.311, 28.978 and 39.289 MPa, respectively.

3.5. TGA analysis of membranes (S1, S2, S3)

To investigate the thermal changes occurring during the sintering process, membrane ingredients were analysed through TGA instrument(Manufacturer: Netzsch, Model: STA449F3A00). Samples were undergone constant heating rate 10°C/min in the presence of argon gas as the carrier gas.

The thermogravimetric analysis (TGA) results of membranes S1, S2 and S3 are depicted in Figure 8. The curves clearly indicate that the main source of weight loss is attributed to the transformation of calcium carbonate (CaCO_3) into carbon dioxide (CO_2). The porosity of the membrane is significantly influenced by the

pathway of CO_2 gas release. Additionally, both membranes S2 and S3 exhibit a similar net weight loss of around 4% for the powder mixture. This observation indicates the membrane weight losses was due to various amounts of calcium carbonate and polyvinyl alcohol (PVA) present in the samples.

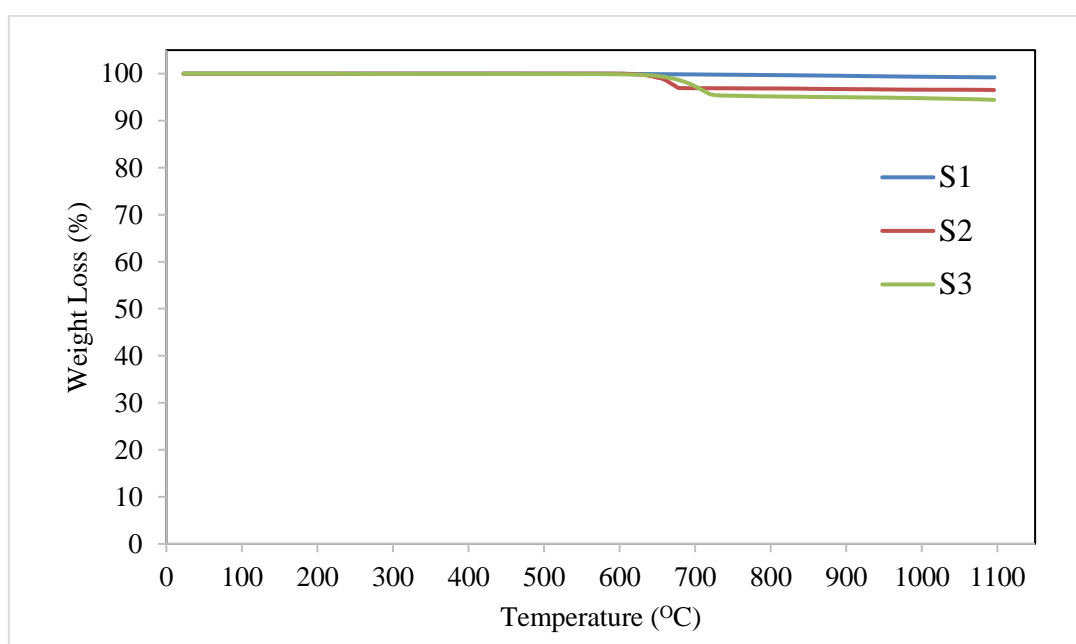


Figure 8: Thermogravimetric analysis of membrane samples mixtures (S1, S2 and S3)

Notably, minimal weight loss is observed across all samples at temperatures exceeding 800 °C, underscoring the need for a minimum sintering temperature higher than 800 °C. In the case of membranes S2 and S3, the significant decrease in mass in the powder mixture at temperatures below 800 °C is caused by the thermal decomposition of CaCO_3 and the evaporation of PVA. In contrast, the TGA plots

obtained for the S1 membrane shows minimum weight loss because of the presence of lower quantity of PVA.

3.6. Water Permeation (S1, S2, S3)

The microfiltration setup used for water permeation and oil-in-water emulsion treatment was illustrated in Fig. 9. This contains Nitrogen cylinder, gas pressure regulator, pressure

gauge, dead end filtration membrane module and bottom weighing balance on top it place a measuring cylinder to collect permeate with respect to time. Each of the fabricated membranes underwent characterization for their hydraulic permeability.

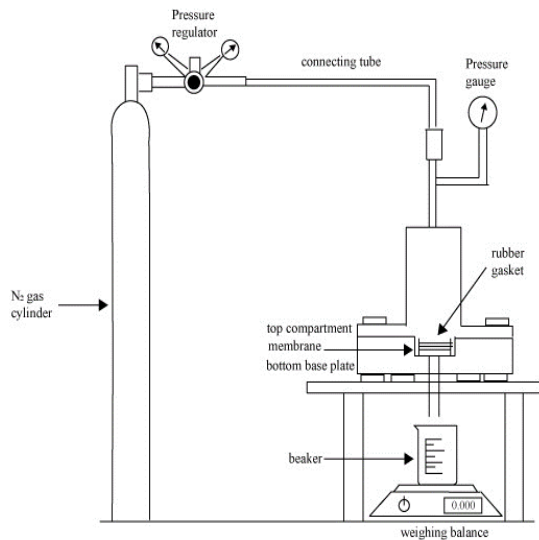


Figure 9: The dead end flow microfiltration setup

Pressure is applied within the range of 30 to 70 kPa, as illustrated in Figure 9 and the pure water flux of the membrane was calculated using Equation 4.

$$J_w = \frac{V_w}{A \times t} \dots\dots\dots \text{Equation (4)}$$

In the equation, A represents the area of the membrane used for filtration, t denotes the duration of filtration, V_w signifies the volume of collected water, and J_w is the water flux.

Figure 10 illustrates the relation between water flux and applied pressure and their variations on pure water flux at various applied pressures that was conducted through water permeation data. The slope of this plot provides the hydraulic permeability value L_h that follows the Darcy's law, same as described in Equation (5).

$$J_w = L_h \Delta P \dots\dots\dots \text{Equation (5)}$$

$$R = \left(\frac{8 \mu_w L L_h \tau}{\varepsilon} \right)^{\frac{1}{2}} \dots\dots\dots \text{Equation (6)}$$

In the equation (6), τ represents the tortuosity of the membrane (assumed as 1 for cylindrical pores), L_h denotes the pure hydraulic permeability, ε represents membrane porosity, R signifies the pore radius, L represents the length of the pore with $l = 0.005$ m, and μ_w denotes the viscosity of water at 25 °C.

The flux of the membranes is observed to be dependent on the applied pressure, increasing with higher applied pressures. The hydraulic permeability of membranes S1, S2, and S3 is calculated to be approximately 11.58×10^{-6} , 10.14×10^{-6} , and 9.19×10^{-6} ($\text{m}^3 / \text{m}^2 \text{ s Pa}$), respectively. Additionally, the average pore sizes of membranes S1, S2, and S3 are determined as 2.12 μm , 1.52 μm , and 1.029 μm , respectively.

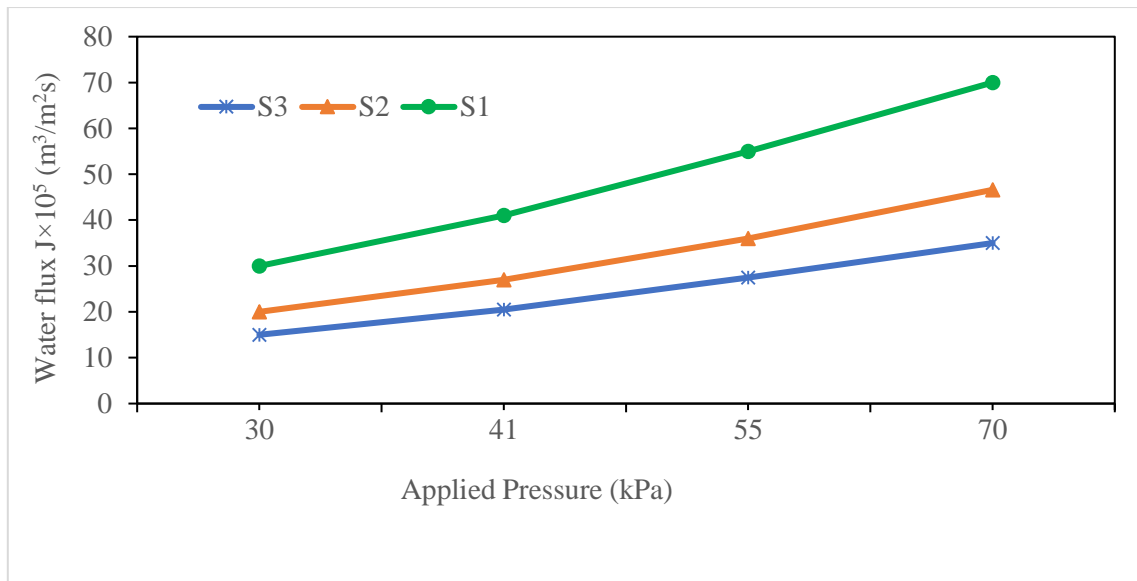


Figure 10: Changes in membrane hydraulic flux under varying applied pressures.

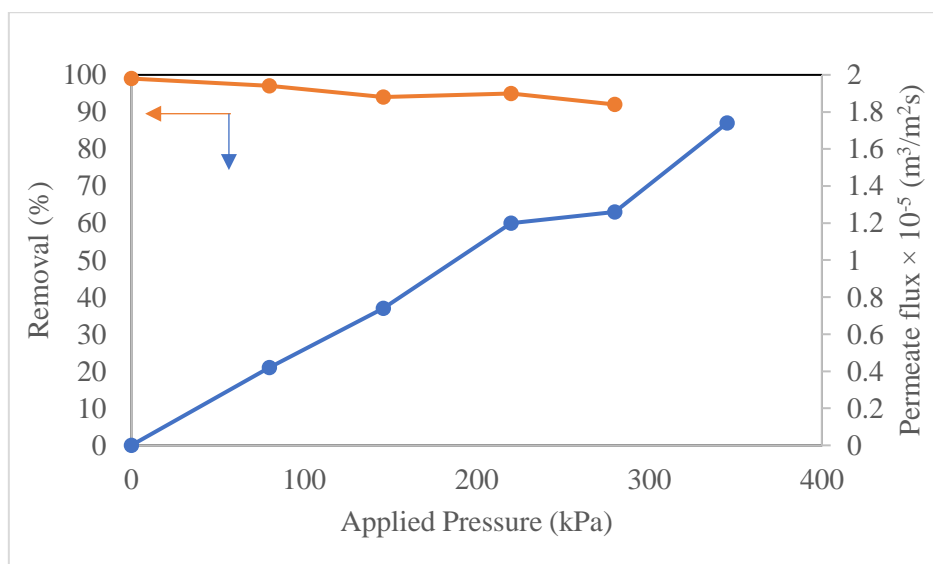


Figure 11: Observing the fluctuation in permeate flux and the oil removal percentage at various applied pressures for the S3 membrane.

Table 5. Comparison of the percentage of oil removal achieved by the membrane with that of other membranes.

Membrane material	Feed concentration (mg/L)	Pore Radius size (μm)	Removal (%)	References
α -Al ₂ O ₃	100	2.1	55	Cui et al. [13]
Al ₂ O ₃	600–11,000	0.16	98	Cui et al. [13]
α - Al ₂ O ₃	150	0.1	61.4	Ebrahimi [15]
α - Al ₂ O ₃ / α - Al ₂ O ₃	5,000	1.0	94.3	Yang et al. [16]
Membrane, S3	200	1.59	98	Present Study

3.7. Oil-in-water emulsion treatment by using membrane S3

Among the crafted membranes, the one featuring the smallest pore size (S3) was specifically chosen for assessing its efficacy in separating oil-water emulsion. Figure 11 depicts the fluctuation in permeate flux and oil removal percentage across different applied pressures, (70 -250 kPa), the primary tested oil sample concentration was 200 mg/L. As expected, the permeation analysis data showed that the removal efficiency reduces with augment of applied pressure it owing to enhanced oil droplet wetting and coalescence, that caused passing of some oil droplets through the membrane with the permeate. These findings are consistent with previous studies [13,16]. Notably, the highest oil rejection rate of 98% is achieved at a relatively lower applied pressure of 70 kPa.

The rejection of oil is calculated using equation (7).

$$R = \left(1 - \frac{C_p}{C_f}\right) \times 100 \dots \dots \dots \text{Equation (7)}$$

Where feed and permeate oil sample concentrations are represented by C_f and C_p respectively.

The driving force across the membrane was increased along enhanced various applied pressures (70-250 kPa) which was helpful to increase the permeate flux. Specifically, the S3 membrane shows significant variation primarily attributed to pore blocking and concentration polarization. In an industrial setting, membranes ideally should combine high purification efficiency with commendable permeate flux. Consequently, the prepared S3 membrane demonstrates superior oil rejection (98–96%) alongside favourable permeate flux. When compared to other membranes (as shown in Table 5). A comparative study concludes that the prepared membranes show better rejection and good permeate flux. Thus, the membrane (S3) derived from fly ash emerges as a promising solution for treating oily wastewater containing oil-in-water emulsions.

4. Conclusions

A range of economically efficient ceramic membranes has been effectively produced using various compositions of raw materials through the uni-axial dry compaction method. These prepared membranes, featuring diverse compositions, exhibit impressive mechanical strength ranging from 26.31 to 39.11 MPa.

When exposed to acid and alkali solutions, the membranes exhibit weight losses of 12% and 6%, respectively, indicating higher stability in alkaline environments. The average pore size of the membranes, determined to be 1.029 μm based on water flux data, is supported by SEM analysis, which measures it to be 1.59 μm . Notably, among all the membranes, S3 shows superior mechanical strength at 39.11 MPa with excellent chemical stability in both acid and base environments. Additionally, membrane S3 displays 39% porosity, water permeability of $9.19 \times 10^{-6} \text{ m}^3 / \text{m}^2 \text{ s Pa}$, and pore size of the membrane is measured at 1.029 μm . This membrane was used to treat oily wastewater with an initial concentration of 200 mg/L, achieving 98% oil removal with a flux $4.20 \times 10^{-8} \text{ m}^3 / \text{m}^2 \text{ s}$ at 80 kPa.

Acknowledgement-

The authors would like to extend our appreciation to the Civil and MME Departments of NIT Bhopal for their assistance in facilitating membrane formation and their support in conducting SEM analysis. The utilization of the UTM in this study was made possible through the generosity of the MME Department. Additionally, Authors extend our

appreciation to the Chemical Engineering Department, NIT Bhopal for providing us with this valuable opportunity

References

1. Benito, J.M., Conesa, A., Rubio, F., & Rodriguez, M.A. (2005). Preparation and characterization of tubular ceramic membranes for treatment of oil emulsions. *Journal of the European Ceramic Society*, 25, 1895–1903.
<https://doi.org/10.1016/j.jeurceramsoc.2004.06.016>
2. Yoshino, Y., Suzuki, T., Nair, B.N., Taguchi, H., & Itoh, N. (2005). Development of tubular substrates, silica based membranes and membrane modules for hydrogen separation at high temperature. *Journal of Membrane Science*, 267, 8–17.
<https://doi.org/10.1016/j.memsci.2005.05.020>
3. Saffaj, N., Persin, M., Younsi, S.A., Albizane, A., Cretin, M., & Larbot, A. (2006). Elaboration and characterization of microfiltration and ultrafiltration membranes deposited on raw support prepared from natural Moroccan clay:

- Application to filtration of solution containing dyes and salts. *Applied Clay Science*, 31, 110–119.
<https://doi.org/10.1016/j.clay.2005.07.002>
4. Rawat, M., & Bulasara, V. K. (2018). Synthesis and characterization of low-cost ceramic membranes from fly ash and kaolin for humic acid separation, *Korean Journal of Chemical Engineering*, 35, 725-733.
<https://doi.org/10.1007/s11814-017-0316-6>
 5. Dong, Y., Hampshire, S., Zhou, J., Lin, B., Ji, Z., Zhang, X., & Meng, G. (2010). Recycling of fly ash for preparing porous mullite membrane supports with titania addition. *Journal of Hazardous Materials*, 180, 173–180.
<https://doi.org/10.1016/j.jhazmat.2010.04.010>
 6. Zou, D., Qiu, M., Chen, X., Drioli, E., & Fan, Y. (2019). One step co-sintering process for low-cost fly ash based ceramic microfiltration membrane in oil-in-water emulsion treatment. *Separation and Purification Technology*, 210, 511-520.
<https://doi.org/10.1016/j.seppur.2018.08.040>
 7. Sing, G., & Bulasara, V.K. (2015). Preparation of low-cost microfiltration membranes from fly ash. *Desalination and Water Treatment*, 53, 1204-1212.
<https://doi.org/10.1080/19443994.2013.855677>
 8. Vasanth, D., Uppaluri, R., & Pugazhenth, G. (2011). Influence of Sintering Temperature on the Properties of Porous Ceramic Support Prepared by Uniaxial Dry Compaction Method Using Low-Cost Raw Materials for Membrane Applications. *Separation Science and Technology*, 46,1241–1249.
<https://doi.org/10.1080/01496395.2011.556097>
 9. Boudaira, B., Harabia, A., Bouzerara, F., & Condom, S. (2009). Preparation and characterization of microfiltration membranes and their supports using kaolin (DD2) and CaCO₃. *Desalination and Water Treatment*, 9, 142–148.
<https://doi.org/10.5004/dwt.2009.764>
 10. Mittal, P., Jana, S., & Mohanty, K. (2011). Synthesis of low-cost hydrophilic ceramic–

- polymeric composite membrane for treatment of oily wastewater. *Desalination*, 282, 54–62.
<https://doi.org/10.1016/j.desal.2011.06.071>
11. Dong, Y.C., Liu, X.Q., Ma, Q.L., & Meng, G.Y. (2006). Preparation of cordierite-based porous ceramic micro-filtration membranes using waste fly ash as the main raw material. *Journal of Membrane Science*, 285, 173–181.
<https://doi.org/10.1016/j.memsci.2006.08.032>
12. Das, B., Chakraborty B., & Barkakati, P. (2017). Separation of oil from oily wastewater using low cost ceramic membrane. *Korean Journal of Chemical Engineering*, 34, 2559-2569.
<https://doi.org/10.1007/s11814-017-0185-z>
13. Cui, J., Zhang, X., Liu, H., Liu, S., & Yeung, K.L. (2008). Preparation and application of zeolite/ceramic microfiltration membranes for treatment of oil contaminated water. *Journal of Membrane Science*, 325, 420–426.
<https://doi.org/10.1016/j.memsci.2008.08.015>
14. Suresh, K., & Pugazhenti, G. (2016). Development of ceramic membranes from low-cost clays for the separation of oil–water emulsion. *Desalination and water treatment*, 57, 1927-1939.
<https://doi.org/10.1080/19443994.2014.979445>
15. Ebrahimi, M., Willershausen, D., Ashaghi, K.S., Engel, L., Placido, L., Mund, P., Bolduan, P., & Czermak, P. (2010). Investigations on the use of different ceramic membranes for efficient oil-field produced water treatment, *Desalination*, 250, 991–996.
<https://doi.org/10.1016/j.desal.2009.09.088>
16. Yang, C., Zhang, G., Xu, N., & Shi, J. (1998). Preparation and application in oil–water separation of $ZrO_2/\alpha-Al_2O_3$ MF membrane. *Journal of Membrane Science*, 142, 235–243.
[https://doi.org/10.1016/S0376-7388\(97\)00336-0](https://doi.org/10.1016/S0376-7388(97)00336-0)